

Coexisting pigeonite and augite are also found in ~12 categories of lunar mare basalts and well-developed skeletal pigeonite mantled by augite is found in Apollo 15 and Apollo 12 pigeonite basalts [6]. All 12 of these basalt groups are magnesium rich, ranging in weight percent MgO from 7.03% to 19.97%, and averaging 10.7% [6]. Like komatiites, the coexisting pyroxenes in the Apollo 12 pigeonite basalts are thought to form by rapid metastable crystallization of a supercooled liquid [7]. Regardless of the specific mechanism that forms skeletal textures and coexisting pigeonite and augite, these features are characteristic of highly magnesian lavas like komatiites.

Discussion: Using ISM data, Mustard et al. [1] estimated the composition of Syrtis Major pyroxenes. According to Mustard et al., the pyroxene compositions represented by their ISM analysis falls in an area of "unusual" composition on the pyroxene quadrilateral, and therefore the data may represent an average composition of augite and pigeonite as intimate exsolution lamella. Telescopic reflectance measurements of several dark regions on Mars are indicative of coexisting pyroxenes, which correlates with the modal mineralogy of Shergotite meteorites, which may have originated from Mars [8]. Comparison with Shergotite meteorites and terrestrial komatiites suggests that exsolution lamella are not required by the results of [1]. If the ISM data represent an average of two pyroxene compositions, then discrete pyroxenes may be implied. Furthermore, if coexisting pyroxenes were detected by the ISM on Syrtis Major, then they may have formed by a mechanism like that previously described for the crystallization of pyroxenes in mafic komatiite and Apollo 12 pigeonite basalts.

Figure 1 shows a pyroxene quadrilateral with the Syrtis Major ISM pyroxene field of [1] superposed over the compositions of pyroxenes found in a pyroxenitic komatiite flow, the Shergotite meteorite, and an Apollo 12 pigeonite basalt. The majority of pyroxenitic komatiite pyroxene analyses do not fall within the ISM field because their source liquid contained relatively little Fe compared to potential martian lavas [e.g., 3,9]. Many individual pyroxene analyses from the Shergotite and the Apollo 12 pigeonite basalt do fall within the ISM field. More importantly, the averaged composition of coexisting pyroxenes in the plotted samples will also fall within the ISM field. These samples perform better than the komatiite because the higher Fe content in these rocks allows greater substitution of Fe in the pyroxene structure as Mg is consumed initially. A crystallization trend is defined that places these pyroxene analy-

ses within and below the ISM field, as seen in Fig. 1. This analysis supports the possibility of komatiite-type lava on the Syrtis Major plateau because these coexisting pyroxenes are indicative of magnesian komatiite-type lava.

An important caveat to the analysis presented here and to that of [1] is that Syrtis Major plateau is composed of a large sand sheet and dune field, with varying degrees of variable fine-grained dust coatings [1]. The question arises whether the materials observed represent locally derived or transported materials. Additionally, if local or distal in origin, certain phases in the Syrtis Major material may have been preferentially concentrated by eolian activity or chemical weathering. The relatively low spatial resolution of ISM (24 km) makes these questions difficult to answer.

A thermal emission spectrometer (TES) with a spectral resolution of 5–10 cm^{-1} , from 5 to 60 μm , and a spatial resolution of 3 km (e.g. the Mars Observer Thermal Emission Spectrometer [10]), would easily reveal the presence and nature of komatiitic lavas on Syrtis Major as indicated by the evidence discussed. In addition, TES-type data could be used to study weathering products and to trace sediment transport paths in an attempt to distinguish primary igneous materials from reworked sediments. Finally, a TES would reveal if Syrtis Major lava composition evolves from peridotitic to basaltic compositions over time as seen in terrestrial komatiites [3].

References: [1] Mustard J. F. et al., (1993) *JGR*, 98, 3387–3400. [2] Takahashi E. (1991) *JGR*, 95, 15941–15954. [3] Arndt N. T. et al. (1977) *J. Pet.*, 18, 319–369. [4] Cameron W. E. and Nisbet E. G. (1982) In *Komatiites* (Arndt N. T. and Nisbet E. G., eds.), George Allen and Unwin, Boston, 29–50. [5] Campbell I. H. and Arndt N. T. (1982) *Geol. Mag.*, 119, 605–610. [6] *BVSP, Basaltic Volcanism Study Project* (1981) Pergamon, New York, 1286 pp. [7] Klein C. et al. (1971) *Proc. LSC 2nd*, 265–284. [8] Straub D. W. et al. (1991) *JGR*, 96, 18819–18830. [9] McGetchin T. R. and Smyth J. R. (1978) *Icarus*, 34, 512–536. [10] Christensen P. R. et al. (1992) *JGR*, 97, 7719–7734

N94-33230

541091 ABS ONLY

MARTIAN DELTAS: MORPHOLOGY AND DISTRIBUTION. J. W. Rice Jr.¹ and D. H. Scott², ¹Department of Geography, Arizona State University, Tempe AZ 85283, USA, ²Astrogeology Branch, U.S. Geological Survey, 2255 N. Gemini Drive, Flagstaff AZ 86001, USA.

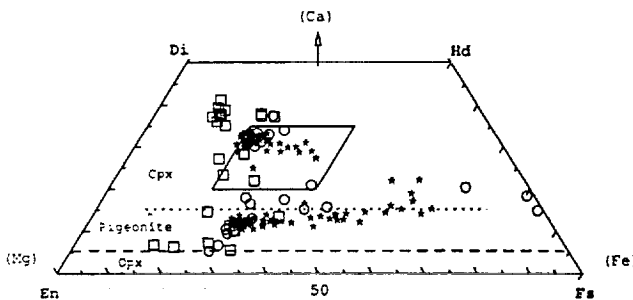


Fig. 1. Pyroxene compositions from Syrtis Major ISM and analogs. ISM field (rhomboid) from [1]; pyroxenitic komatiite data (squares) provided by D. P. Reyes, [sample DPY-10, unpublished data, Reyes, 1993]; and Apollo 12 pigeonite basalt (circles) and Shergotite meteorite (stars) data from [6].

The identification of deltas on Mars has been an enigma over the years for planetary geologists. However, recent detailed mapping (1:500,000 scale) has revealed numerous examples of martian deltas. We will document and describe the location and morphology of these deltas.

Deltas are alluvial regions composed of sediment deposited in relatively still water (lakes, bays, seas) at river mouths. Deposition on deltas occurs when river velocity is reduced upon entering standing bodies of water. Factors that contribute to delta morphology are river regime, coastal processes, structural stability, and climate [1].

The largest delta systems on Mars are located near the mouths of Maja, Maumee, Vedra, Ma'adim, Kasei, and Brazos Valles. There are also several smaller-scale deltas emplaced near channel mouths situated in Ismenius Lacus, Memnonia, and Arabia.

Delta morphology will be used to reconstruct type, quantity, and sediment load size transported by the debouching channel systems

[2,3]. For example, arcuate deltas are deposited by bed load or mixed load systems that bring large quantities of coarse material to the coastline as opposed to the elongate (birdfoot) deltas composed of large quantities of fine sediment deposited by a combination of suspended load and mixed load rivers. Methods initially developed for terrestrial systems will be used to gain information on the relationships between martian delta morphology, river regime, and coastal processes.

References: [1] Morgan J. P. (1970) *SEPM*, 15, 31-47. [2] Axelsson V. (1967) *Geogr. Ann.*, 49, 2-127. [3] Galloway W. E. (1975) *Houston Geol. Soc.*, 87-98.

N94-33231

54-91 ABS ONLY

CARBONATE FORMATION ON MARS: LATEST EXPERIMENTS. S. K. Stephens¹, D. J. Stevenson¹, G. R. Rossman¹, and L. F. Keyser², ¹Division of Geological and Planetary Sciences, 170-25, California Institute of Technology, Pasadena CA 91125, USA, ²Earth and Space Sciences Division, 183-901, Jet Propulsion Laboratory, California Institute of Technology, Pasadena CA 91109, USA.

Introduction: Laboratory simulations of martian CO₂ storage address a fundamental question about martian climate history: Could carbonate formation have reduced CO₂ pressure from a hypothetical >1 bar to the present 7 mbar in ≤3-4 b.y.? We address this problem with experiments and analysis [1,2] designed to verify and improve previous [3,4] kinetic measurements, reaction mechanisms, and product characterizations. Our theoretical modeling [5,6] has sought to improve existing models of martian CO₂ history [7-10], which generally assume an early CO₂ greenhouse atmosphere (questioned by Kasting [11]).

Experimental Results: A sensitive manometer monitored the pressure drop (PD) of CO₂ due to uptake by powdered silicate for periods of 3 to 100+ days. Initially we focused on monomineralic, crystalline samples, but more recently we ran basaltic glass (see Table 1). Grinding was done in a tungsten-carbide shatterbox. Di1 was not treated further, and all other monomineralic samples were

heated at 120°C for ~1 day after sitting in weak acetic acid for 1+ days. Bas was simply heated. Runs were performed at warm (25°C) and cold (-25°C) temperatures, about 1 bar CO₂ pressure, and specific surface areas of ~1 m²/g (~1 μm particles). Experiments included "vapor" (H₂O premixed with CO₂, for ~1-10 monolayer coverage), "damp" (H₂O pipetted onto powder before soaking in), and "wet" (m_{H₂O} ~ m_{sample}) runs.

BET specific surface areas were determined for Di1 and Bas, and quantitative results are given for experiments using these starting compositions (Table 2). Pressure drops (ΔP) for Di1 and Bas show rapid short-term (~1 day) CO₂ uptake and considerably slower long-term ΔP (Figs. 1 and 2). We know the changes are not due to H₂O adsorption since there is always sufficient water to maintain $\lambda_{\text{vap}}(\text{H}_2\text{O})$. However, we assume the short-term signal reflects CO₂ adsorption (consistent with previous measurements [7,12] and confirmed by desorption experiments). Curves for Di2, O11, and O12 are qualitatively similar to those for Di1, whereas Qtz and Plag show near-zero short-term ΔP and very slow long-term signal—indistinguishable from a leak (<10¹¹ mol/m²/s).

Discussion: Thermodynamic calculations [13] suggest that reactions should form carbonates from diopside and olivine, and possibly plagioclase, at martian P and T. PD results can be classified into three groups: diopsides and olivines, quartz and plagioclase, and basalt. Bas takes up more CO₂ than monomineralic, crystalline diopside, and olivine, despite the fact that it is probably >50% feldspar and quartz (i.e., relatively unreactive), suggesting a role for glass (vs. crystalline mineral).

No long-term ΔP was expected for Qtz (no cations), although adsorption was anticipated, while with Plag we expected a possible long-term signal, and again the absence of an adsorption effect was puzzling. One explanation involves the progressive polymerization of silicate tetrahedra: olivine (isolated tetrahedra) and pyroxene (chains) vs. feldspar and quartz (three-dimensional frameworks). The structure of olivine and diopside may make it easier for cations to physically adsorb (and/or chemically bond with) anions.

Also puzzling is the result of an X-ray photoelectron spectroscopy (XPS) analysis performed on Di2 exposed to similar P(CO₂) and H₂O vapor conditions as the PD experiment with Di1 (vapor)

TABLE 1. Minerals and rocks used for experimental samples.

Sample	Approximate Composition	Sample Description	Locale
Diopside 1 [Di1]	CaMgSi ₂ O ₆	Bulk, broken crystals, ~5% impurities	Dog Lake, Quebec
Diopside 2 [Di2]	CaMgSi ₂ O ₆	Green, euhedral crystals, <2% impurities	Rajasthan, India
Olivine 1 [O11]	Mg ₉₈ Fe ₀₂ SiO ₄ [Forsterite 98%]	Bulk, broken crystals, ~5% impurities	Gabbs, Nevada
Olivine 2 [O12]	Mg ₈₈ Fe ₁₂ SiO ₄	Translucent green pebbles (crystals). <2% impurities	San Carlos, Arizona
Quartz [Qtz]	SiO ₂	Clear, euhedral crystal, <1% impurities	Mt. Ida, Arkansas
Plagioclase [Plag]	Ab ₁ An ₉ [Ab = NaAlSi ₃ O ₈ , An = CaAl ₂ Si ₂ O ₈]	Clear, euhedral crystal <1% impurities	Ponderosa Mine, Oregon
Basalt [Bas]	Tholeiite [50 wt% SiO ₂ , 13% Al ₂ O ₃ , 12% FeO, 9% MgO, 11% CaO]	~98 wt% black glass, ~0.3 wt% dissolved H ₂ O ~1 wt% crystals, 1991 lava flow, quenched in air	Kilauea, Hawaii